RFC3 drives the proliferation, migration, invasion and angiogenesis of colorectal cancer cells by binding KIF14

RONG YU[1], XINXIN WU[2], FANG QIAN[3] and QIAN YANG[4]

[1]Department of General Surgery, Quzhou Kecheng People's Hospital, Quzhou, Zhejiang 324000; [2]Department of General Surgery, Yancheng Dafeng Hospital of Traditional Chinese Medicine, Yancheng, Jiangsu 224110; [3]Department of Radiology, Wuxi Xinwu Hospital of Traditional Chinese Medicine, Wuxi, Jiangsu 214000; [4]Department of Radiology, Maternal and Child Health Hospital of Huaiyin District, Huai'an, Jiangsu 223300, P.R. China

Received August 3, 2023; Accepted January 26, 2024

DOI: 10.3892/etm.2024.12510

Abstract. Colorectal cancer (CRC) is a deadly and aggressive type of cancer that has a high fatality rate. The expression levels of replication factor C subunit 3 (RFC3) and kinesin family member 14 (KIF14) have been reported to be increased in CRC. The current study aimed to explore the effects of RFC3 on the malignant behaviors of CRC cells and its possible underlying mechanism involving KIF14. RFC3 and KIF14 expression levels in CRC tissues were analyzed using TNMplot database and Gene Expression Profiling Interactive Analysis database bioinformatics tools. RFC3 and KIF14 levels in CRC cells were examined using reverse transcription-quantitative PCR and western blotting. Cell Counting Kit-8 and 5-ethynyl-2'-deoxyuridine assays were performed to assess cell proliferation. Cell apoptosis was determined using flow cytometric analysis. Wound healing and Transwell assays were adopted for the evaluation of cell migration and invasion. Tube formation assay in human umbilical vein endothelial cells was used to measure angiogenesis. Western blotting analysis was performed to determine the expression of apoptosis-, migration- and angiogenesis-associated proteins. Additionally, bioinformatics tools predicted the co-expression and interaction of RFC3 and KIF14, which was verified by a co-immunoprecipitation assay. RFC3 displayed elevated expression in CRC tissues and cells, and depletion of RFC3 halted the proliferation, migration, invasion and angiogenesis, while increasing the apoptosis of CRC cells; this was accompanied by changes in the expression levels of related proteins. In addition, RFC3 bound to KIF14 and interference with RFC3 reduced KIF14 expression. Moreover, KIF14 upregulation reversed the effects of RFC3 depletion on the aggressive cellular behaviors in CRC. In conclusion, RFC3 might interact with KIF14 to function as a contributor to the malignant development of CRC.

Correspondence to: Dr Qian Yang, Department of Radiology, Maternal and Child Health Hospital of Huaiyin District, 116 Beijing East Road, Huaiyin, Huai'an, Jiangsu 223300, P.R. China
E-mail: shine_doctor1352@163.com

Key words: colorectal cancer, kinesin family member 14, replication factor C subunit 3, angiogenesis, invasion

Introduction

Colorectal cancer (CRC) is an aggressive tumor that originates in the inner wall of the large intestine. Overall, according to recent statistics, it has been estimated that ~153,000 cases of CRC will be reported in 2023, of which >1/3 may die of this disease, thus accounting for ~10% of all cancer-associated mortalities (1,2). Despite the favorable prognosis of patients with early-stage CRC after the application of comprehensive and evidence-based therapies, such as a combination of surgery, chemotherapy, targeted therapy and/or radiation (3), most patients with CRC at advanced stages will develop recurrence and distant metastasis in the course of the disease, resulting in a poor outcome (4). Growing evidence has indicated that epigenetic alterations participate in the process of CRC (5,6). Therefore, insight into the mechanism underlying the malignant development of CRC and any effective biomarkers may result in the identification of novel therapeutic regimes for CRC.

Replication factor C (RFC) is a component of the eukaryotic DNA polymerase involved in DNA replication, DNA damage repair and checkpoint control (7,8). As a subunit of the RFC family, RFC subunit 3 (RFC3), originally purified from HeLa cells, has been determined to play an essential role in the *in vitro* replication of Simian virus 40 (9). Previous evidence has expounded that RFC3 is highly expressed in lung adenocarcinoma (10), ovarian carcinoma (11), hepatocellular carcinoma (12) and triple-negative breast cancer cells (13), and that it drives the aggressive biological phenotypes of cells, such as migration and invasion (13). All of these findings have identified RFC3 as a potential oncogene. Furthermore, RFC3 is upregulated in CRC tissues and RFC3 alteration shows worse disease-free survival of patients with CRC (14). However, the effect of RFC3 on CRC cells *in vitro* remains to be elucidated.

Kinesin, a cytoskeletal motor, is responsible for the intracellular transport of organelles and vesicles along microtubules (15). As reported, kinesin extensively participates in a variety of diseases (16,17). Belonging to the kinesin-3 family,

the functions of kinesin family member 14 (KIF14) are also dependent on microtubules. Notably, KIF14 has been proposed as a tumor promoter in multiple human malignancies, including cervical cancer (18), gastric cancer (19) and retinoblastoma (20). Notably, Wang *et al* has suggested that KIF14, targeted by microRNA (miR)-200c, activates Akt to elicit pro-proliferation activities in CRC (21). The present study planned to investigate the possible interaction between RFC3 and KIF14.

The present research was designed to identify the effects of RFC3 and KIF14 on the proliferation, migration, invasion and angiogenesis of CRC. Furthermore, the possible interaction between RFC3 and KIF14 was explored to reveal the potential mechanism. This study may expose a novel therapeutic target for CRC treatment.

Materials and methods

Bioinformatics tools. The TNMplot database (https://tnmplot.com/analysis/) was used to analyze the expression levels of RFC3 and KIF14 in CRC (tumor) tissues and normal tissues. Gene Expression Profiling Interactive Analysis (GEPIA) database (http://gepia.cancer-pku.cn) were also employed to evaluate the expression levels of RFC3 and KIF14 in colon adenocarcinoma (COAD) tissues and normal tissues (the original image downloaded from GEPIA database displayed in the form of log transformation). The survival analyses were performed using the KM-plot (http://kmplot.com/analysis) database. Coexpedia database (https://www.coexpedia.org/) and Biogrid database (https://thebiogrid.org/) were used to predict the co-expression between RFC3 and KIF14.

Cell culture and treatment. CRC cell lines (SW620, HCT8 and HCT 116) and human umbilical vein endothelial cells (HUVECs) were all procured from BeNa Culture Collection (Beijing Beina Chunglian Institute of Biotechnology), while the human normal intestinal epithelial cell line (HIEC-6) was purchased from Shanghai Yaji Biological Technology Co., Ltd. HCT8 and HCT 116 cells were subjected to cultivation in RPMI-1640 medium (Wisent Biotechnology), while the SW620 cell line was maintained in DMEM (Wisent Biotechnology). The aforementioned media were both supplemented with 10% fetal bovine serum (FBS; Wisent Biotechnology) under the atmosphere of 5% CO_2 at 37˚C. Opti-MEM (Invitrogen; Thermo Fisher Scientific, Inc.) supplemented with 10 ng/ml epidermal growth factor (EGF), 4% FBS, 20 mM HEPES and 10 mM GlutaMAX was prepared for the incubation of HIEC-6 cells, while endothelial cell medium (Shenzhen Aipunuo Biotechnology Co., Ltd.) containing 1% ECGS and 10% FBS was prepared for the cultivation of HUVECs. When cell confluence reached 80%, the cells were digested with 0.25% trypsin (Beyotime Institute of Biotechnology) and centrifuged at 800 x g for 5 min at room temperature. After discarding the supernatant, the cells were resuspended in PBS and adjusted to a cell density of $3x10^5$/ml. The cell suspension (1 ml) was collected and seeded in a six-well culture plate, which was placed overnight in an incubator under the same conditions as those aforementioned.

Transfection. SW620 cells ($3x10^5$ cells/well) were inoculated onto six-well plates and cultured at 37˚C with 5% CO_2 until the cell confluence reached 85%. RFC3-labeled small interfering RNAs (siRNAs) (si-RFC3-1, 5'-GCATTGAAGATATTTGCCACGTGTT-3'; si-RFC3-2, 5'-GAGATAATAATGAAGGGCCTTCTCT-3') or the nonsense siRNA (siRNA-NC, 5'-GCAAAGTAGTTACGATTCATGATCT-3') provided by Vigene Biosciences (Charles River Laboratories, Inc.), and the KIF14 pcDNA3.1 overexpression plasmid (Ov-KIF14) or empty vector pcDNA3.1 plasmid (Ov-NC) synthesized by Tsingke Biological Technology, were transfected into SW620 cells using Lipofectamine 2000 (Invitrogen; Thermo Fisher Scientific, Inc.) as per the manufacturer's instructions. At 48 h after transfection, the cells were harvested to conduct the subsequent experiments.

Reverse transcription-quantitative PCR (RT-qPCR). Following total RNA isolation from several CRC cell lines (SW620, HCT8 and HCT 116) or HIEC-6 cells using TRIzol® reagent (Invitrogen; Thermo Fisher Scientific, Inc.), cDNA was acquired with the aid of the First-strand cDNA Synthesis Kit (Thermo Fisher Scientific, Inc.) according to the manufacturer's protocol. Then, SYBR green PCR Master mix (KAPA Biosystems; Roche Diagnostics) was adopted for qPCR analysis, using cDNA as a template. The PCR reaction conditions consisted of 95˚C for 3 min, followed by 40 cycles of 95˚C for 30 sec and 60˚C for 30 sec. Relative RFC3 and KIF14 expression levels were calibrated in terms of the $2^{-\Delta\Delta Cq}$ approach (22). GAPDH functioned as a normalization gene. The primer sequences were as follows: RFC3, forward 5'-GTGGACAAGTATCGGCCCTG-3' and reverse 5'-TGATGGTCCGTACACTAACAGAT-3'; KIF14, forward 5'-CCTCACCCACAGTAGCCGA-3' and reverse 5'-AAGTGCCAATCTACCTACAGGA-3'; GAPDH forward 5'-TGTGGGCATCAATGGATTTGG-3' and reverse 5'-ACACCATGTATTCCGGGTCAAT-3'.

Western blotting. RIPA lysis buffer (Beyotime Institute of Biotechnology) was added to cells in each well and placed on ice for 20 min. After centrifugation at 800 x g at 4˚C for 10 min, the supernatant was obtained to detect the total protein concentration using a bicinchoninic acid kit (Beyotime Institute of Biotechnology). Then, the equal amount of proteins (40 μg/lane) was separated by 10% SDS-PAGE and transferred to PVDF membranes. After being pre-coated with 5% BSA (Beyotime Institute of Biotechnology) for 1 h at room temperature, the membranes were successively labeled with RFC3 (cat. no. ab182143; 1/1,000; Abcam), KIF14 (cat. no. ab71155; ½,000; Abcam), B cell lymphoma 2 (BCL2; cat. no. ab182858; 1/2,000; Abcam), BCL2-associated X (Bax; cat. no. ab32503; 1/1,000; Abcam), cleaved caspase 3 (cat. no. ab32042; 1/500; Abcam), matrix metallopeptidase 2 (MMP2; cat. no. ab92536; 1/1,000; Abcam), matrix metallopeptidase 9 (MMP9; cat. no. ab76003; 1/1,000; Abcam), vascular EGF (VEGF; cat. no. sc-57496; 1/1,000; Santa Cruz Biotechnology, Inc.) and VEGF receptor 1 (VEGFR1; cat. no. ab32152; 1/1,000; Abcam) primary antibodies overnight at 4˚C, followed by incubation with goat anti-rabbit IgG (cat. no. ab97051; 1/2,000; Abcam) or goat anti-mouse IgG (cat. no. ab6789; ½,000; Abcam) for 1 h at room temperature. The blots were visualized using the enhanced chemiluminescence detection reagent (Shanghai Yeasen Biotechnology Co., Ltd.) and densitometric analysis

was performed with ImageJ software (version 1.49; National Institutes of Health).

Cell Counting Kit-8 (CCK-8) assay. After transfection, SW620 cells were injected into 96-well plates (1,000 cells/well). With the help of a microplate reader (Shenzhen Reagent Technology Co., Ltd.), the OD 450 nm value was estimated, after each well was loaded with 10 μl CCK-8 solution (Beyotime Institute of Biotechnology) for 2 h of incubation.

5-Ethynyl-2'-deoxyuridine (EDU) staining. Cell proliferation was measured using an EDU staining kit (Beijing Solarbio Science & Technology Co., Ltd.). Transiently transfected SW620 cells (5,000 cells/well) were seeded into 96-well plates supplemented with 50 μM EDU for 2 h in compliance with the manufacturer's protocol. Following 30 min of immobilization with 4% paraformaldehyde at 37˚C and 10 min of permeation with 1% Triton X-100 at 37˚C, cells were stained with DAPI for 30 min at room temperature. Images were prepared for observation under a fluorescence microscope (Leica Microsystems GmbH).

Flow cytometric analysis. After the indicated treatment, SW620 cells in each group were routinely digested with 0.25% trypsin (Beyotime Institute of Biotechnology) for 10 min at room temperature, followed by washing with PBS three times and centrifugation at 2,000 x g for 3 min at 4˚C. Then, the supernatant was discarded, and the cell concentration was adjusted to $5x10^5$ cells per sample. Cells were mixed with 5 μl Annexin V-FITC (Multisciences (Lianke) Biotech Co., Ltd.) and 5 μl propidium iodide (Multisciences (Lianke) Biotech Co., Ltd.) for 15 min at room temperature. Analysis of cell apoptosis was performed using BD FACSAria flow cytometry (BD Biosciences). FlowJo vX.0.7 software (FlowJo LLC) was used to assess the rates of apoptosis.

Wound healing assay. SW620 cells were inoculated in six-well plates ($4x10^5$ cells/well). After cells reached 90% confluence, a straight wound was gently made on the surface of the plate via the application of a 200-μl pipette tip The suspended cells were then submerged in DMEM deprived of serum. A light microscope (Leica Microsystems GmbH) was used to detect the wound area at 0 and 24 h. The extent of wound healing was calculated as follows: Migration (%)=(wound area at 0 h-wound area at 24 h)/wound area at 0 h.

Transwell assay. The upper sides of Transwell inserts (8 μm; Corning, Inc.) coated with Matrigel (BD Biosciences) at 37˚C for 1 h were loaded with SW620 cells ($5x10^4$ cells/well) in DMEM deprived of serum, whereas 500 μl DMEM containing 10% FBS was added to the undersides as a chemoattractant. After 24 h incubation at 37˚C, the remaining cells were cleared while the invaded cells were stained with crystal violet for 10 min at room temperature and images were captured under a light microscope.

Tube formation assay. Prior to the implementation of the tube formation assay, conditioned medium (CM) was harvested after the culture medium of SW620 cells in six-well plates was changed to DMEM deprived of serum. Subsequently, HUVECs ($1x10^5$) were spread onto 96-well plates precoated with Matrigel at 37˚C for 1 h in CM. Tubules were observed under an inverted light microscope and subjected to analysis with ImageJ software (version 1.49; National Institutes of Health).

Co-immunoprecipitation (Co-IP) assay. The Co-IP assay was conducted using the Co-IP kit [cat. no. abs9649-50T; Aibixin (Shanghai) Biotechnology Co., Ltd.]. Briefly, SW620 cells were lysed on ice for 30 min in radioimmunoprecipitation assay (RIPA) lysis buffer (Beyotime Institute of Biotechnology). Next, 2 μg RFC3 (cat. no. 11814-1-AP; Proteintech Group, Inc.), KIF14 (cat. no. ab71155; Abcam) or goat anti-rabbit IgG (the negative control; cat. no. ab172730; Abcam) antibodies were added to 500 μg SW620 cell lysates and incubated overnight at 4˚C. Subsequently, 50 μg protein A magnetic beads (cat. no. #sc-2003; Santa Cruz Biotechnology, Inc.) were added for capturing the complexes of RFC3 and KIF14. After the IP reaction, 50 μg protein G/A agarose beads were centrifuged at 1,000 x g for 3 min at 4˚C to the bottom of the tube. The supernatant was then carefully absorbed, and the agarose beads were washed three times with PBS. A total of 15 μl 2X SDS sample buffer was finally added for boiling at 100˚C for 5 min. The immunoprecipitants were analyzed by western blotting.

Statistical analyses. The data are presented as the mean ± standard deviation from three independent experiments adopting GraphPad Prism 8 software (GraphPad Software, Inc.; Dotmatics). One-way ANOVA followed by Tukey's test was used to analyze data. $P<0.05$ was considered to indicate a statistically significant difference.

Results

RFC3 displays upregulated expression in CRC cells. RFC3 expression in CRC tissues was analyzed by using TNMplot and GEPIA databases. As shown in Fig. 1A and B, RFC3 was highly expressed in CRC tumor tissues compared with the normal tissues. To figure out the specific role of RFC3 in CRC, RFC3 expression was detected by RT-qPCR and western blotting. As shown in Fig. 1C and D, RFC3 mRNA and protein expression levels were both significantly increased in SW620, HCT8 and HCT 116 cells compared with those in the HIEC-6 cell line. Notably, SW620 cells exhibited the most prominently elevated RFC3 expression, and were thus selected for the follow-up experiments.

RFC3 depletion diminishes the proliferation and aggravates the apoptosis of CRC cells. To specify the effects of RFC3 on the aggressive process of CRC, RFC3 expression was silenced prior to the implementation of loss-of-function experiments. After transfection with si-RFC3-1/2, there was a significant decrease in both RFC3 mRNA and protein expression levels compared with the siRNA-NC group (Fig. 2A and B). In particular, the interference efficacy of si-RFC3-1 was more apparent than that of si-RFC3-2, and was thus applied to the subsequent experiments.

As determined by CCK-8 assay, SW620 cell viability was significantly suppressed by depletion of RFC3 (Fig. 2C). Also, the experimental data from EDU staining illuminated that the number of EDU-positive cells was reduced when RFC3 was

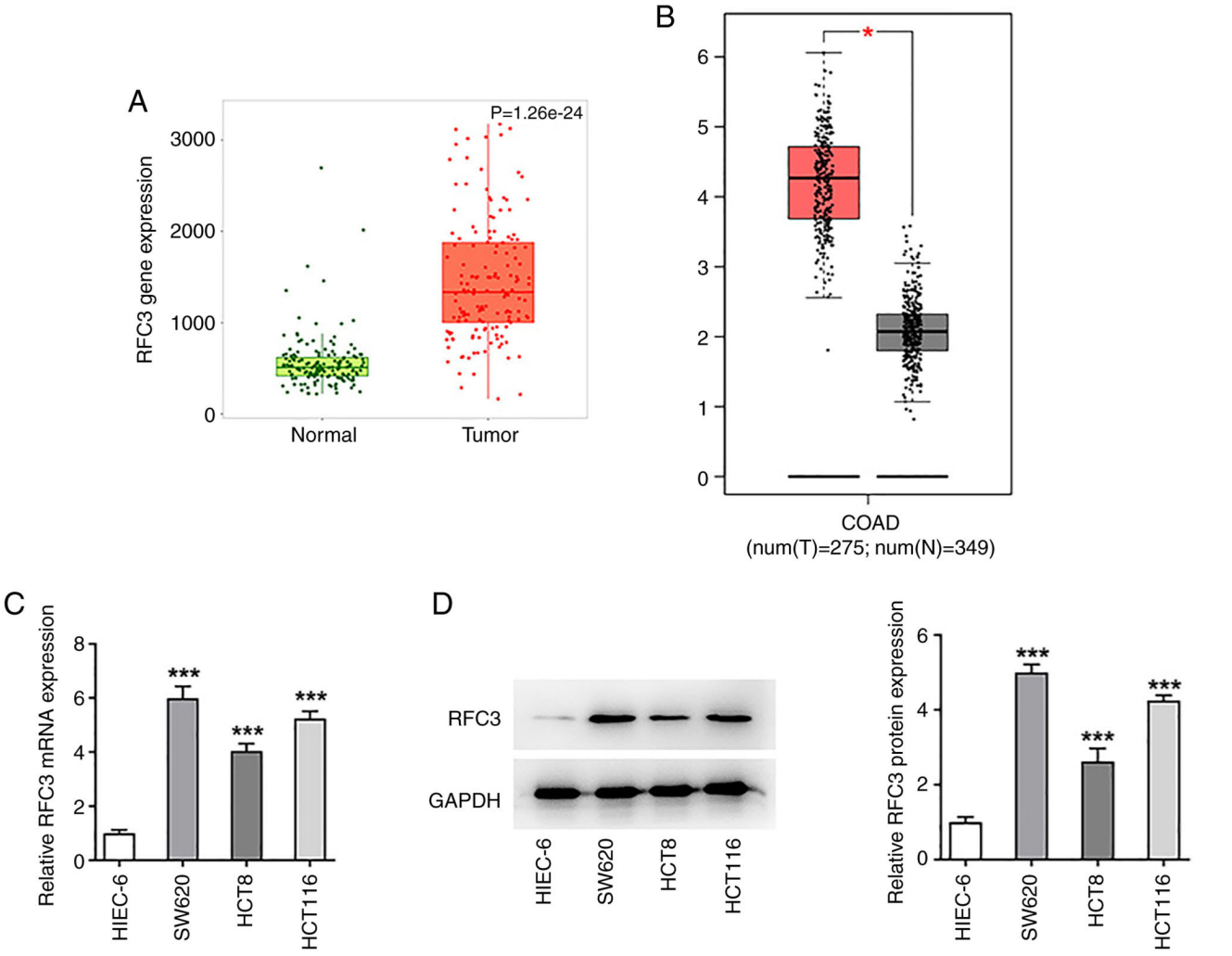

Figure 1. RFC3 displays upregulated expression in CRC cells. (A) RFC3 expression in normal and CRC tumor tissues of patients was analyzed using the TNMplot tool. (B) Box plot illustrates RFC3 expression level in 275 COAD tissues (red) vs. normal 349 tissues (gray) derived from the GEPIA database. *P<0.05. (C) Reverse transcription-quantitative PCR and (D) western blotting analysis of RFC3 expression. ***P<0.001 vs. HIEC-6 group. CRC, colorectal cancer; RFC3, replication factor C subunit 3; COAD, colon adenocarcinoma.

downregulated (Fig. 2D). Furthermore, the effects of RFC3 on the apoptosis of SW620 cells were evaluated. By contrast, through flow cytometric analysis, it was revealed that RFC3 inhibition resulted in a significant increase in the apoptotic rate of SW620 cells (Fig. 3A and B). In addition, the expression levels of proteins involved in apoptosis were examined, and it was discovered that BCL2 expression was decreased, while Bax and Cleaved caspase3 expression levels were increased after RFC3 was depleted (Fig. 3C). To sum up, RFC3 interference protected against CRC cell proliferation and contributed to CRC cell apoptosis.

RFC3 depletion obstructs CRC cell migration, invasion and angiogenesis. Wound healing and Transwell assays were used to measure SW620 cell migration and invasion, respectively. The results revealed that the migratory and invasive capacities of SW620 cells were both significantly decreased by the depletion of RFC3 compared with the siRNA-NC (Fig. 4A and B). Western blotting also revealed that depletion of RFC3 significantly reduced the protein expression levels of metastasis-associated MMP2 and MMP9 compared with the siRNA-NC (Fig. 4C). Tube formation assays demonstrated that the tube formation capacity of HUVECs was attenuated in the CM from RFC3-silenced SW620 cells (Fig. 4D), which was accompanied by the significantly reduced protein expression levels of angiogenesis-related VEGF and VEGFR1 (Fig. 4E). Overall, RFC3-knockdown decreased the migration, invasion and angiogenesis of CRC cells.

RFC3 protein interacts with KIF14 protein. The Coexpedia and Biogrid databases were used predict the co-expression between RFC3 and KIF14. As predicted by the Coexpedia database, RFC3 and KIF14 were co-expressed (Fig. 5A). The potential binding of the RFC3 protein to the KIF14 protein was also shown in the Biogrid database (Fig. 5B). Additionally, TNMplot and GEPIA databases revealed that KIF14 expression was significantly upregulated in CRC tissues compared with the normal tissues (Fig. 5C-D). Higher KIF14 expression predicted the decreased survival in patients with CRC (Fig. 5E). Though western blotting, KIF14 protein expression was revealed to be significantly depleted after RFC3 was knocked down (Fig. 5F). The results of Co-IP revealed that

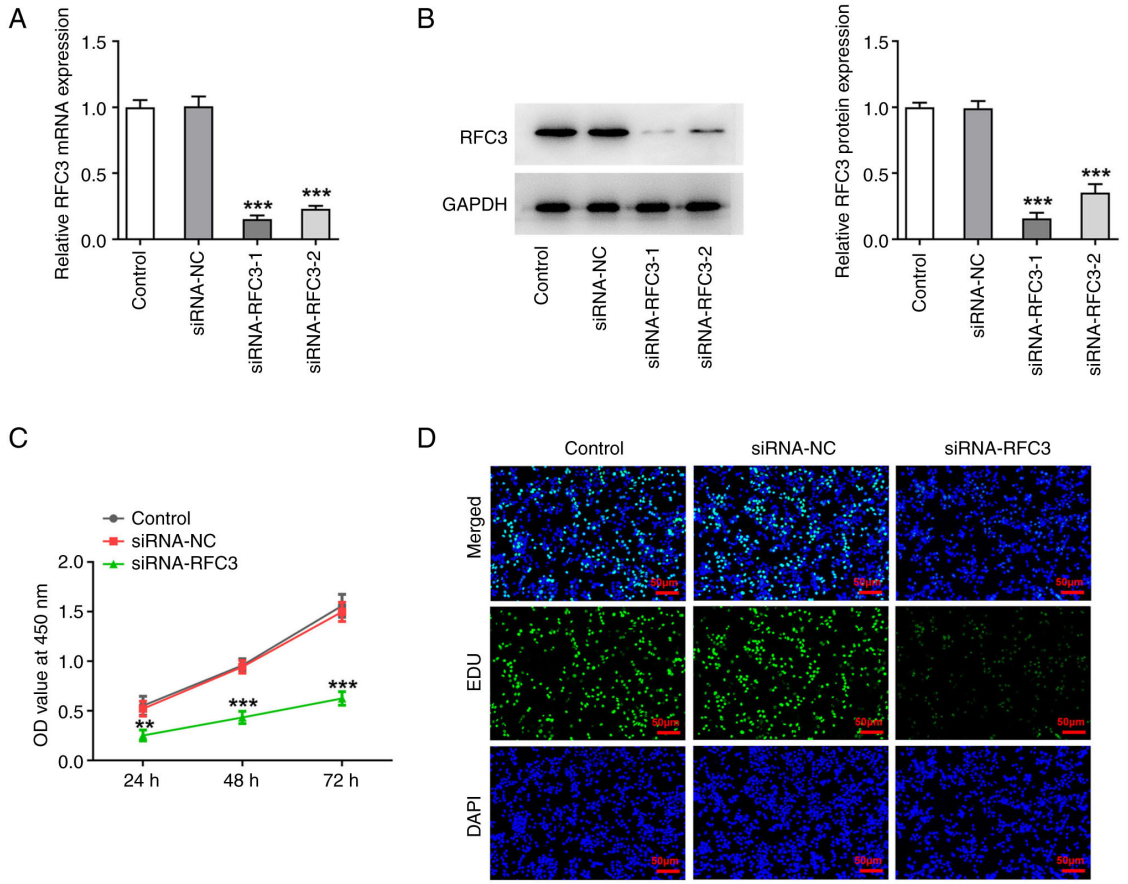

Figure 2. RFC3 depletion diminishes the proliferation of SW620 cells. (A) Reverse transcription-quantitative PCR and (B) western blotting examined the transfection efficacy of siRNA-RFC3-1/2. (C) Cell viability was assessed using the Cell Counting Kit-8 method. (D) EDU staining (magnification, x200) measured cell proliferation. **P<0.01, ***P<0.001 vs. siRNA-NC group. RFC3, replication factor C subunit 3; siRNA, small interfering RNA; NC, negative control.

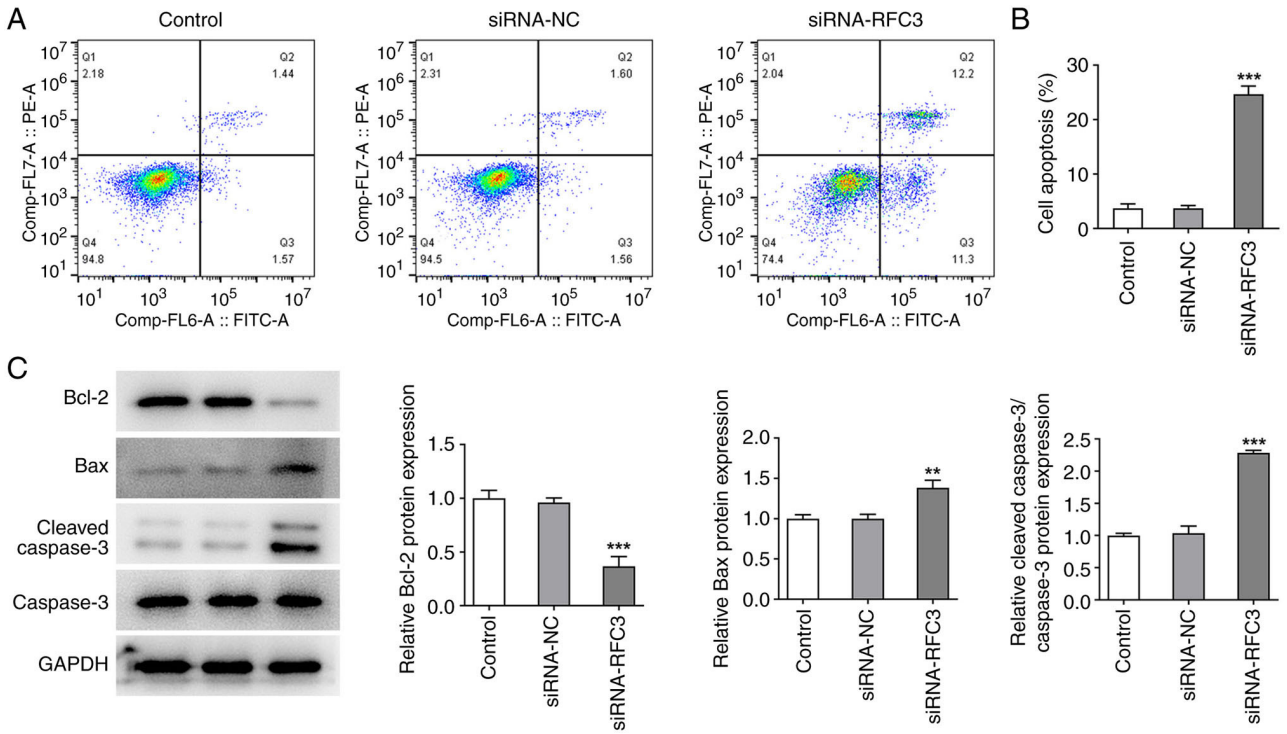

Figure 3. RFC3 depletion aggravates the apoptosis of SW620 cells. (A) Flow cytometric analysis of cell apoptosis and (B) quantification. (C) Western blotting tested the expression of apoptosis-associated proteins. **P<0.01, ***P<0.001 vs. siRNA-NC group. RFC3, replication factor C subunit 3; siRNA, small interfering RNA; NC, negative control.

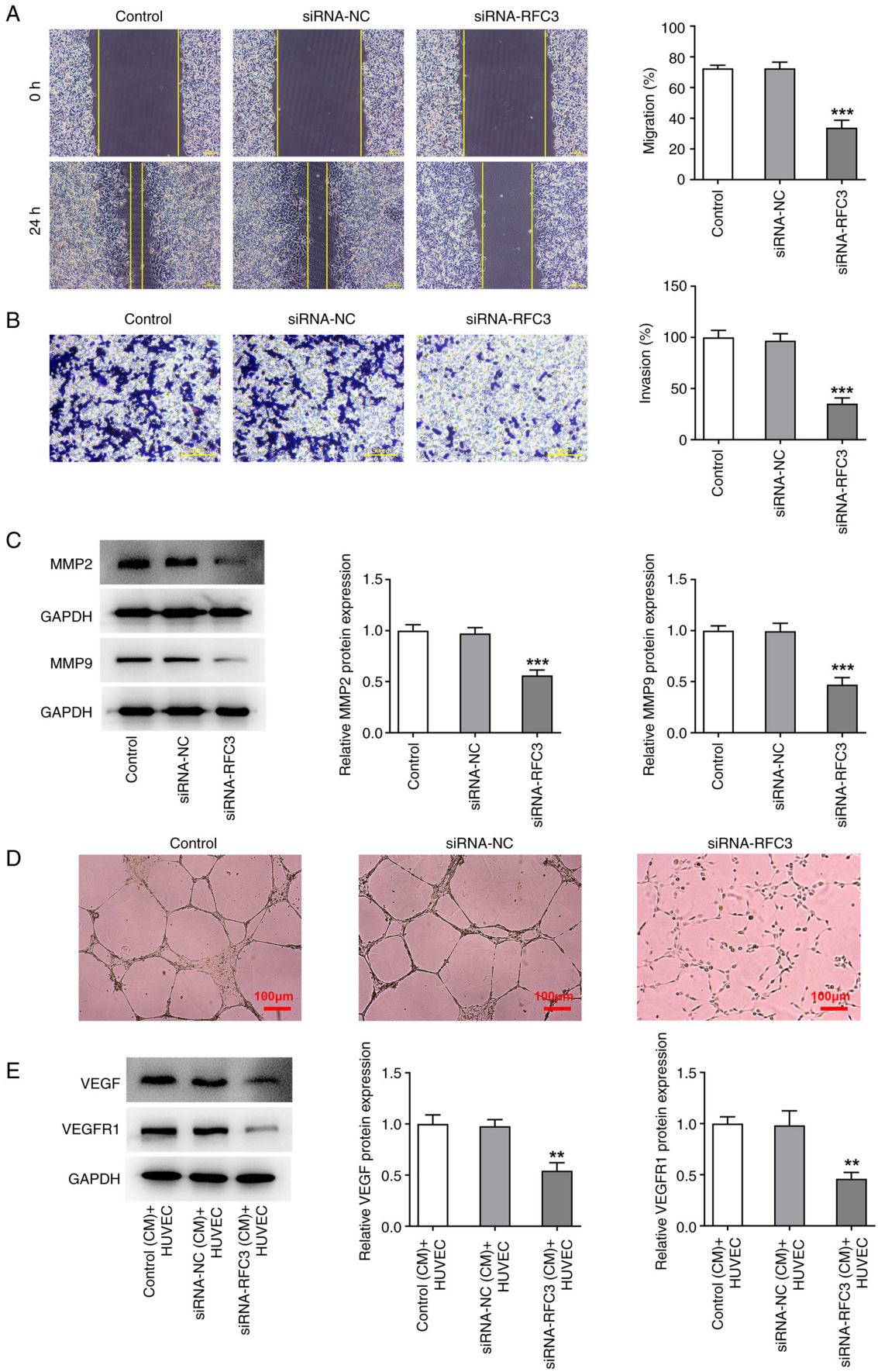

Figure 4. RFC3 depletion obstructs SW620 cell migration, invasion and angiogenesis. (A) Wound healing (magnification, x100) and (B) Transwell assays (magnification, x200) estimated the migration and invasion of cells. (C) Western blotting tested the expression of metastasis-associated proteins. ***P<0.001 vs. siRNA-NC group. (D) Tube formation assay (magnification, x100) assessed HUVECs angiogenesis in the conditioned medium of SW620 cells. (E) Western blotting tested the expression of angiogenesis-associated proteins. **P<0.01 vs. siRNA-NC (CM) + HUVEC group. RFC3, replication factor C subunit 3; siRNA, small interfering RNA; NC, negative control; MMP, matrix metallopeptidase; VEGF, vascular epidermal growth factor; VEGFR, VEGF receptor.

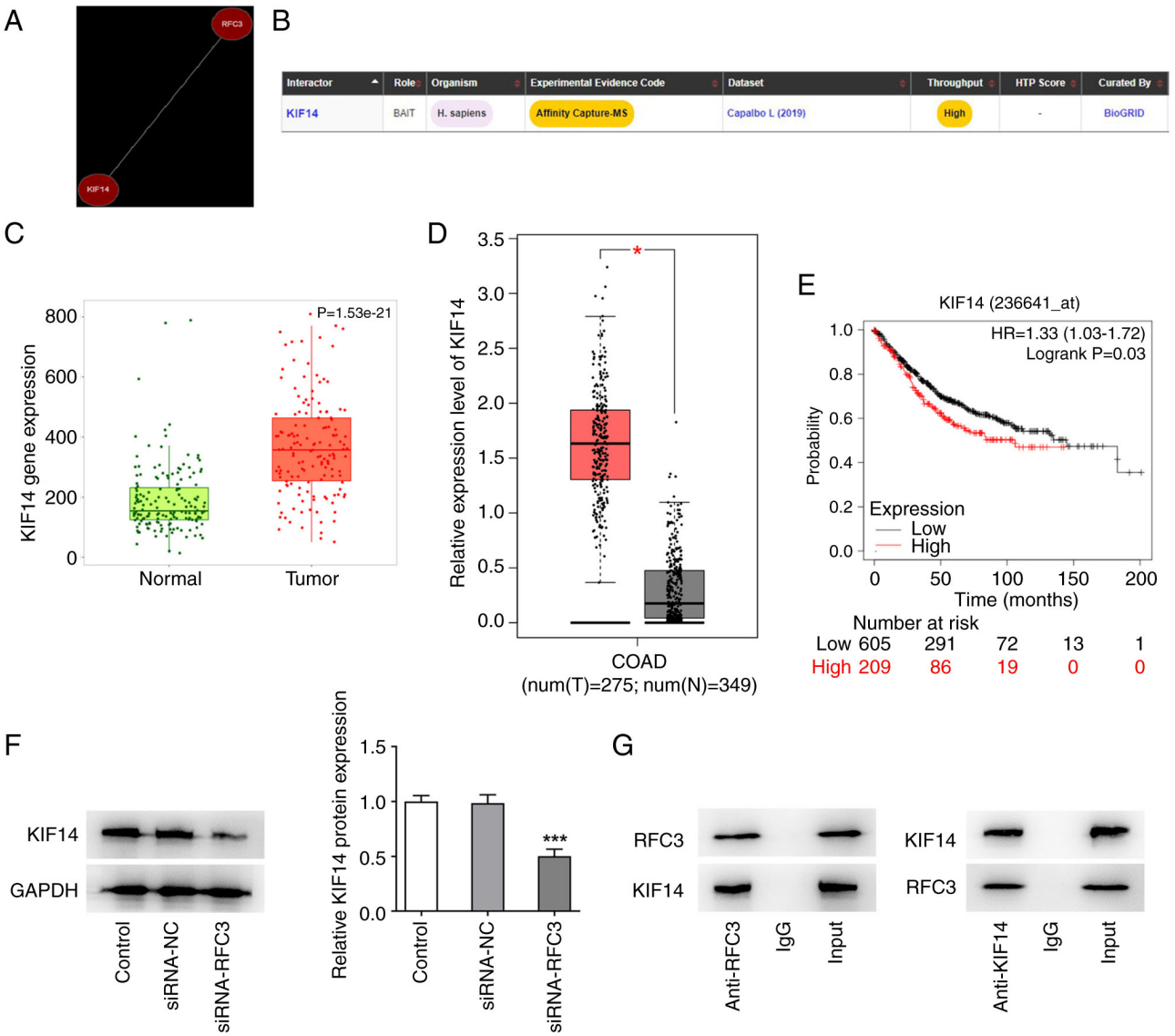

Figure 5. RFC3 protein interacts with KIF14 protein. (A) Coexpedia database predicted the co-expression of RFC3 and KIF14. (B) Biogrid database predicted the relationship between RFC3 and KIF14. (C) KIF14 expression in normal and CRC tumor tissues of patients was analyzed using the TNMplot tool. (D) The box plot illustrated KIF14 expression level in 275 COAD tissues vs. normal 349 tissues derived from the GEPIA database. *P<0.05. (E) Long-term survival between patients with low and high KIF14 expression levels, according to KM-plot database. ***P<0.001 vs. siRNA-NC group. (G) Co-immunoprecipitation assay validated the interaction between RFC3 and KIF14. RFC3, replication factor C subunit 3; siRNA, small interfering RNA; NC, negative control; KIF14, kinesin family member 14; CRC, colorectal cancer; COAD, colon adenocarcinoma; GEPIA, Gene Expression Profiling Interactive Analysis.

both RFC3 and KIF14 were expressed in the input group. KIF14 protein was revealed to exist in the anti-RFC3 group and RFC3 protein was revealed to exist in the anti-KIF14 group. However, IgG could not pull down RFC3 and was used to rule out false-positive results. This suggested that RFC3 potentially interacted with KIF14 (Fig. 5G).

RFC3 insufficiency downregulates KIF14 to hamper CRC cell proliferation and exacerbate CRC cell apoptosis. With the aim of determining whether the interaction between RFC3 and KIF14 was involved in the progression of CRC, KIF14 expression was markedly increased after transfection with Ov-KIF14 (Fig. 6A and B). The results of the CCK-8 assay revealed that RFC3 depletion blocked the viability of SW620 cells, which was then improved after KIF14 was overexpressed (Fig. 6C). As illustrated in Fig. 6D, the suppressed SW620 cell proliferation induced by RFC3 interference was increased again when KIF14 was upregulated. Concurrently, the number of apoptotic SW620 cells was noticeably enhanced due to RFC3 inhibition, which was then reversed by KIF14 elevation (Fig. 7A and B). Similarly, the expression levels of BCL2, and the augmented expression levels of Bax and Cleaved caspase3 in RFC3-silenced SW620 cells were both reversed by upregulation of KIF14 (Fig. 7C). All of these results suggested that the effects of RFC3 knockdown on the proliferation and apoptosis of CRC cells were reversed by KIF14 elevation.

RFC3 insufficiency downregulates KIF14 to halt the migration, invasion and angiogenesis of CRC cells. Moreover, the restrained SW620 cell migration and

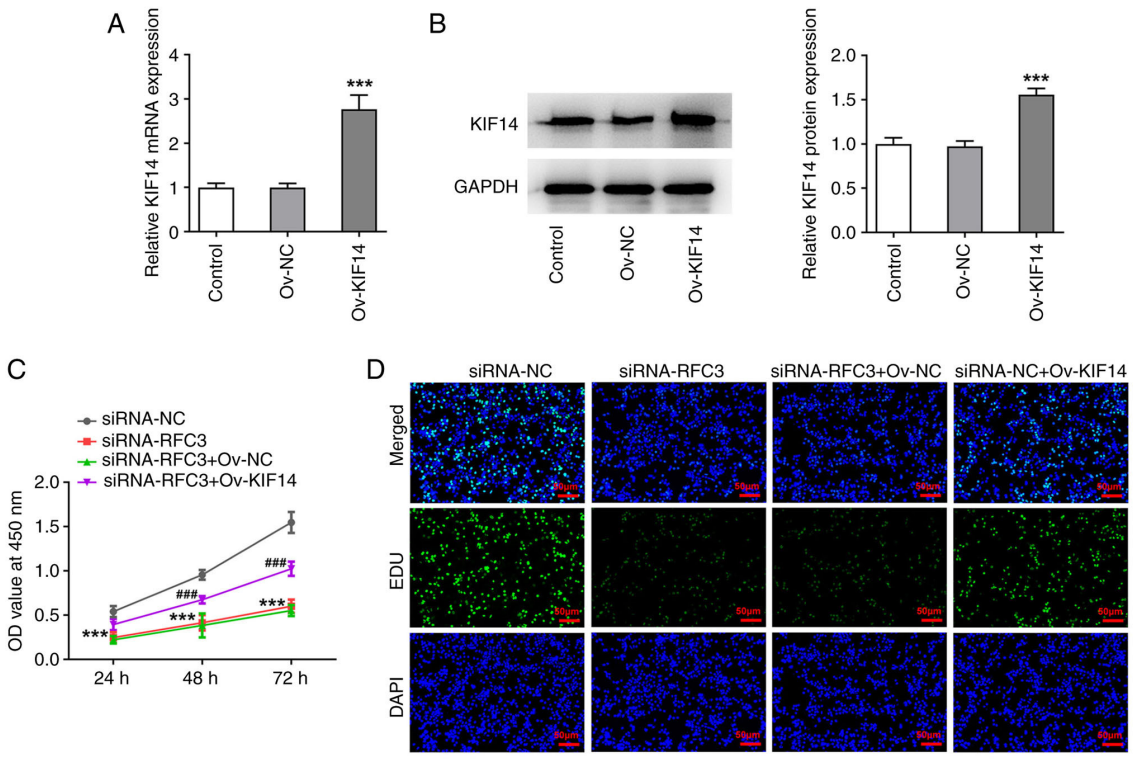

Figure 6. Downregulation of KIF14 mediated by RFC3 insufficiency decreases the proliferation of SW620 cells. (A) Reverse transcription-quantitative PCR and (B) western blotting examined the transfection efficacy of Ov-KIF14 plasmids. ***P<0.001 vs. Ov-NC group. (C) Cell viability was assessed using the Cell Counting Kit-8 method. (D) EDU staining (magnification, x200) measured cell proliferation. ***P<0.001 vs. siRNA-NC group; ###P<0.001 vs. siRNA-RFC3 + Ov-NC group. RFC3, replication factor C subunit 3; Ov, overexpression; NC, negative control; KIF14, kinesin family member 14.

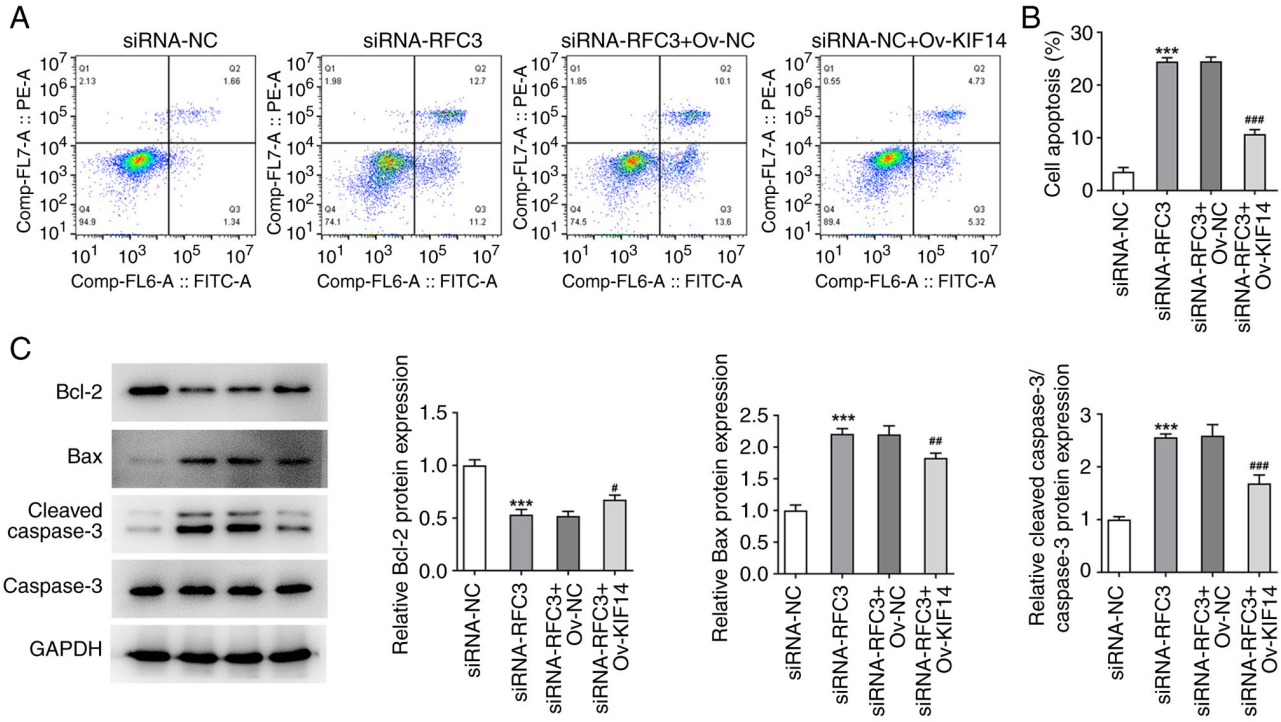

Figure 7. Downregulation of KIF14 mediated by RFC3 insufficiency increases the apoptosis of SW620 cells. (A) Flow cytometric analysis of apoptosis and (B) quantification. (C) Western blotting tested the expression of apoptosis-associated proteins. ***P<0.001 vs. siRNA-NC group; #P<0.05, ##P<0.01, ###P<0.001 vs. siRNA-RFC3 + Ov-NC group. RFC3, replication factor C subunit 3; Ov, overexpression; NC, negative control; KIF14, kinesin family member 14.

invasion mediated by RFC3 depletion were facilitated again by overexpression of KIF14 (Fig. 8A and B), which was also evidenced by the increased expression levels of MMP2 and MMP9 in RFC3-silenced SW620 cells transfected with

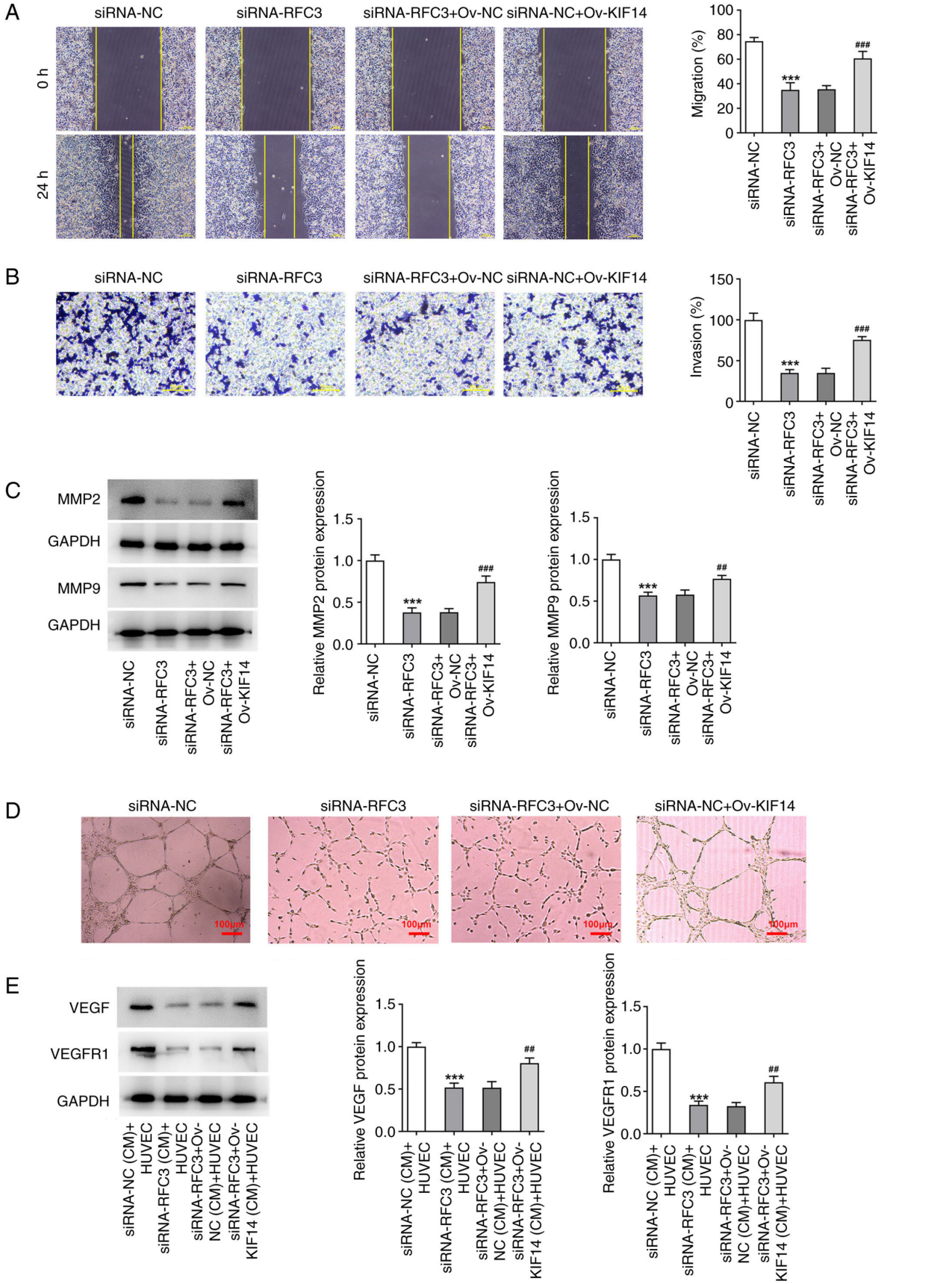

Figure 8. Downregulation of KIF14 mediated by RFC3 insufficiency decreases the migration, invasion and angiogenesis of SW620 cells. (A) Wound healing (magnification, x100) and (B) Transwell assays (magnification, x200) estimated the migration and invasion of cells. (C) Western blotting tested the expression of metastasis-associated proteins. ***P<0.001 vs. siRNA-NC group; ##P<0.01, ###P<0.001 vs. siRNA-RFC3 + Ov-NC group. (D) Tube formation assay (magnification, x100) assessed HUVEC angiogenesis in the conditioned medium of SW620 cells. (E) Western blotting tested the expression of angiogenesis-associated proteins. ***P<0.001 vs. siRNA-NC (CM) + HUVEC group; ##P<0.01 vs. siRNA-RFC3 + Ov-NC (CM) + HUVEC group. RFC3, replication factor C subunit 3; Ov, overexpression; NC, negative control; KIF14, kinesin family member 14; siRNA, small interfering RNA; VEGF, vascular epidermal growth factor; VEGFR, VEGF receptor.

Ov-KIF14 (Fig. 8C). Furthermore, RFC3 downregulation reduced HUVECs tube formation, and depleted VEGF and VEGFR1 expression levels in the CM of SW620 cells, which was then partially restored by elevation of KIF14 (Fig. 8D and E). Taken together, the inhibitory role of RFC3 depletion in CRC cell migration, invasion and angiogenesis was counteracted by KIF14.

Discussion

Metastasis and angiogenesis are considered the major drivers of CRC, which results from the transition of then normal colonic epithelium to adenoma (23,24). In addition, a stepwise accumulation of genetic and epigenetic alterations is involved in the process of CRC (25). In the present study, RFC3 expression was elevated in CRC cells, whereas RFC3 deficiency decreased the proliferation, migration, invasion and angiogenesis, while stimulating the apoptosis, of SW620 cells. Moreover, RFC3 was revealed to potentially interact with KIF14.

RFC family members have been demonstrated to participate in the biological behaviors of cancer cells, including CRC (26,27). Dysregulation of RFC3 has been detected in multiple tumors. For instance, RFC3 downregulation reduces the invasion, migration and epithelial-mesenchymal transition of lung adenocarcinoma and breast cancer cells (10,13). Lin *et al* elaborated that RFC3 is upregulated in CRC and RFC3 mutations may affect the outcome of patients with CRC (14). Consistent with this finding, RFC3 was revealed to be highly expressed in CRC cells in the current study. Functional experiments illuminated that after RFC3 was depleted following transfection with si-RFC3-1/2, the viability and proliferation of CRC cells were decreased, whereas the apoptosis of SW620 cells was aggravated, accompanied by a decrease in anti-apoptotic BCL2 expression and an increase in pro-apoptotic Bax and Cleaved caspase 3 expression. Knockdown of RFC3 resulted in a reduction in the migratory and invasive capacities, as well as the expression levels of metastasis-related MMP2 and MMP9 in SW620 cells.

Through supplying the blood with oxygen and nutrients dependent on new vessels, angiogenesis may exert a profound impact on the formation and progression of solid tumors (28). Besides, aberrant regulation of angiogenesis is deemed as one of the most significant mechanisms involved in tumor invasion and metastasis (29). VEGF represents a growth factor with important pro-angiogenic activity, which functions through binding with VEGFR1, a member of the VEGF family (30). High expression of VEGF and blood vessel formation are closely related to the invasion, metastasis and poor prognosis of CRC (31-33). In the present study, the impacts of RFC3 on angiogenesis in CRC were also assessed, and it was demonstrated that HUVEC tube formation was obstructed in the CM from SW620 cells transfected with si-RFC3, which was also evidenced by the decline in VEGF and VEGFR1 protein expression, suggesting the anti-angiogenic role of RFC3 absence in CRC.

Based on Coexpedia and Biogrid databases, RFC3 was predicted to be co-expressed with KIF14 and to bind with KIF14. As reported by Ji *et al*, KIF14 may be implicated in the miR-17-3p/PLCD1 regulatory process in colon cancer by interacting with the PLCD1 protein (34). Through the present investigation, it was revealed that KIF14 expression was also decreased when RFC3 was downregulated. Mechanistic assays also identified the binding of the RFC3 protein with the KIF14 protein. Inhibition of KIF14 has been supported to suppress angiogenesis in esophageal squamous cell carcinoma and glioma (35,36). Moreover, KIF14 expression is altered in CRC tissues and is associated with the clinical outcome of patients with CRC, as well as the cell cycle, DNA replication and DNA repair in CRC (37). Additionally, growing evidence has documented that KIF14 is overexpressed in CRC and acts as a tumor promoter by accelerating cell proliferation (21,34). The present study indicated that after KIF14 was overexpressed, the suppressive role of RFC3 deficiency in cell proliferation, migration, invasion and angiogenesis, and its stimulatory role in apoptosis in CRC were partially counteracted.

In conclusion, RFC3 exhibited increased expression in CRC cells and disruption of RFC3 may halt the development of CRC. To the best of our knowledge, this is the first report corroborating that RFC3 modulates the cellular events in CRC by interacting with KIF14. Therefore, RFC3 may function as a molecular marker for CRC and silencing RFC3 may be valued as a potential therapeutic modality for CRC. The present study only discussed the role of RFC3 and KIF14 in the malignant phenotypes of SW620 cells. The more CRC cell lines validation and further *in vivo* animal experiments will be performed in the future investigation to support the conclusion obtained in this study. In addition, the lack of a relationship between RFC3 expression levels and survival in patients with CRC is another limitation of the current study.

Acknowledgements

Not applicable.

Funding

No funding was received.

Authors' contributions

RY and XW were responsible for the methodology, data curation and writing the original draft preparation. FQ was responsible for the statistical analysis, validation and writing, reviewing and editing the manuscript. QY was responsible for the conceptualization, project administration, supervision and funding acquisition. All the authors read and approved the final manuscript. RY and QY confirm the authenticity of all the raw data.

Availability of data and material

The datasets used and/or analyzed during the current study are available from the corresponding author on reasonable request.

Ethics approval and consent to participate

Not applicable.

Patient consent for publication

Not applicable.

Competing interests

The authors declare that they have no competing interests.

References

1. Siegel RL, Wagle NS, Cercek A, Smith RA and Jemal A: Colorectal cancer statistics, 2023. CA Cancer J Clin 73: 233-254, 2023.
2. Sung H, Ferlay J, Siegel RL, Laversanne M, Soerjomataram I, Jemal A and Bray F: Global cancer statistics 2020: GLOBOCAN estimates of incidence and mortality worldwide for 36 cancers in 185 countries. CA Cancer J Clin 71: 209-249, 2021.
3. Simard J, Kamath S and Kircher S: Survivorship guidance for patients with colorectal cancer. Curr Treat Options Oncol 20: 38, 2019.
4. Fakih MG: Metastatic colorectal cancer: Current state and future directions. J Clin Oncol 33: 1809-1824, 2015.
5. Jung G, Hernández-Illán E, Moreira L, Balaguer F and Goel A: Epigenetics of colorectal cancer: Biomarker and therapeutic potential. Nat Rev Gastroenterol Hepatol 17: 111-130, 2020.
6. Essa HYS, Kusaf G, Yuruker O and Kalkan R: Epigenetic alteration in colorectal cancer: A biomarker for diagnostic and therapeutic application. Glob Med Genet 9: 258-262, 2022.
7. Sakato M, O'Donnell M and Hingorani MM: A central swivel point in the RFC clamp loader controls PCNA opening and loading on DNA. J Mol Biol 416: 163-175, 2012.
8. Majka J and Burgers PM: The PCNA-RFC families of DNA clamps and clamp loaders. Prog Nucleic Acid Res Mol Biol 78: 227-260, 2004.
9. Xia S, Xiao L, Gannon P and Li X: RFC3 regulates cell proliferation and pathogen resistance in Arabidopsis. Plant Signal Behav 5: 168-170, 2010.
10. Gong S, Qu X, Yang S, Zhou S, Li P and Zhang Q: RFC3 induces epithelial-mesenchymal transition in lung adenocarcinoma cells through the Wnt/β-catenin pathway and possesses prognostic value in lung adenocarcinoma. Int J Mol Med 44: 2276-2288, 2019.
11. Shen H, Cai M, Zhao S, Wang H, Li M, Yao S and Jiang N: Overexpression of RFC3 is correlated with ovarian tumor development and poor prognosis. Tumour Biol 35: 10259-10266, 2014.
12. Yao Z, Hu K, Huang H, Xu S, Wang Q, Zhang P, Yang P and Liu B: shRNA-mediated silencing of the RFC3 gene suppresses hepatocellular carcinoma cell proliferation. Int J Mol Med 36: 1393-1399, 2015.
13. He ZY, Wu SG, Peng F, Zhang Q, Luo Y, Chen M and Bao Y: Up-Regulation of RFC3 promotes triple negative breast cancer metastasis and is associated with poor prognosis via EMT. Transl Oncol 10: 1-9, 2017.
14. Lin K, Zhu X, Luo C, Bu F, Zhu J and Zhu Z: Data mining combined with experiments to validate CEP55 as a prognostic biomarker in colorectal cancer. Immun Inflamm Dis 9: 167-182, 2021.
15. Niwa S: Kinesin superfamily proteins and the regulation of microtubule dynamics in morphogenesis. Anat Sci Int 90: 1-6, 2015.
16. Morfini G, Schmidt N, Weissmann C, Pigino G and Kins S: Conventional kinesin: Biochemical heterogeneity and functional implications in health and disease. Brain Res Bull 126(Pt 3): 347-353, 2016.
17. Lucanus AJ and Yip GW: Kinesin superfamily: Roles in breast cancer, patient prognosis and therapeutics. Oncogene 37: 833-838, 2018.
18. Zhang J, Buranjiang G, Mutalifu Z, Jin H and Yao L: KIF14 affects cell cycle arrest and cell viability in cervical cancer by regulating the p27(^{Kip1}) pathway. World J Surg Oncol 20: 125, 2022.
19. Yang Z, Li C, Yan C, Li J, Yan M, Liu B, Zhu Z, Wu Y and Gu Q: KIF14 promotes tumor progression and metastasis and is an independent predictor of poor prognosis in human gastric cancer. Biochim Biophys Acta Mol Basis Dis 1865: 181-192, 2019.
20. O'Hare M, Shadmand M, Sulaiman RS, Sishtla K, Sakisaka T and Corson TW: Kif14 overexpression accelerates murine retinoblastoma development. Int J Cancer 139: 1752-1758, 2016.
21. Wang ZZ, Yang J, Jiang BH, Di JB, Gao P, Peng L and Su XQ: KIF14 promotes cell proliferation via activation of Akt and is directly targeted by miR-200c in colorectal cancer. Int J Oncol 53: 1939-1952, 2018.
22. Livak KJ and Schmittgen TD: Analysis of relative gene expression data using real-time quantitative PCR and the 2(-Delta Delta C(T)) method. Methods 25: 402-408, 2001.
23. Nappi A, Nasti G, Romano C, Berretta M and Ottaiano A: Metastatic colorectal cancer: Prognostic and predictive factors. Curr Med Chem 27: 2779-2791, 2020.
24. Chan E: Angiogenesis in colorectal cancer: Antibodies. Cancer J 22: 179-181, 2016.
25. Coppedè F: The role of epigenetics in colorectal cancer. Expert Rev Gastroenterol Hepatol 8: 935-948, 2014.
26. Li Y, Gan S, Ren L, Yuan L, Liu J, Wang W, Wang X, Zhang Y, Jiang J, Zhang F and Qi X: Multifaceted regulation and functions of replication factor C family in human cancers. Am J Cancer Res 8: 1343-1355, 2018.
27. Hu T, Shen H, Li J, Yang P, Gu Q and Fu Z: RFC2, a direct target of miR-744, modulates the cell cycle and promotes the proliferation of CRC cells. J Cell Physiol 235: 8319-8333, 2020.
28. Al-Ostoot FH, Salah S, Khamees HA and Khanum SA: Tumor angiogenesis: Current challenges and therapeutic opportunities. Cancer Treat Res Commun 28: 100422, 2021.
29. Bielenberg DR and Zetter BR: The contribution of angiogenesis to the process of metastasis. Cancer J 21: 267-273, 2015.
30. Melincovici CS, Boşca AB, Şuşman S, Mărginean M, Mihu C, Istrate M, Moldovan IM, Roman AL and Mihu CM: Vascular endothelial growth factor (VEGF)-key factor in normal and pathological angiogenesis. Rom J Morphol Embryol 59: 455-467, 2018.
31. Wang R, Ma Y, Zhan S, Zhang G, Cao L, Zhang X, Shi T and Chen W: B7-H3 promotes colorectal cancer angiogenesis through activating the NF-κB pathway to induce VEGFA expression. Cell Death Dis 11: 55, 2020.
32. Dakowicz D, Zajkowska M and Mroczko B: Relationship between VEGF family members, their receptors and cell death in the neoplastic transformation of colorectal cancer. Int J Mol Sci 23: 3375, 2022.
33. Freire Valls A, Knipper K, Giannakouri E, Sarachaga V, Hinterkopf S, Wuehrl M, Shen Y, Radhakrishnan P, Klose J, Ulrich A, *et al*: VEGFR1(+) metastasis-associated macrophages contribute to metastatic angiogenesis and influence colorectal cancer patient outcome. Clin Cancer Res 25: 5674-5685, 2019.
34. Ji J and Fu J: MiR-17-3p facilitates aggressive cell phenotypes in colon cancer by targeting PLCD1 through affecting KIF14. Appl Biochem Biotechnol 195: 1723-1735, 2023.
35. Zhao Q, Chen S and Chen L: LETM1 (leucine zipper-EF-hand-containing transmembrane protein 1) silence reduces the proliferation, invasion, migration and angiogenesis in esophageal squamous cell carcinoma via KIF14 (kinesin family member 14). Bioengineered 12: 7656-7665, 2021.
36. Xu H, Zhao G, Zhang Y, Jiang H, Wang W, Zhao D, Yu H and Qi L: Long non-coding RNA PAXIP1-AS1 facilitates cell invasion and angiogenesis of glioma by recruiting transcription factor ETS1 to upregulate KIF14 expression. J Exp Clin Cancer Res 38: 486, 2019.
37. Neska-Długosz I, Buchholz K, Durślewicz J, Gagat M, Grzanka D, Tojek K and Klimaszewska-Wiśniewska A: Prognostic impact and functional annotations of KIF11 and KIF14 expression in patients with colorectal cancer. Int J Mol Sci 22: 9732, 2021.